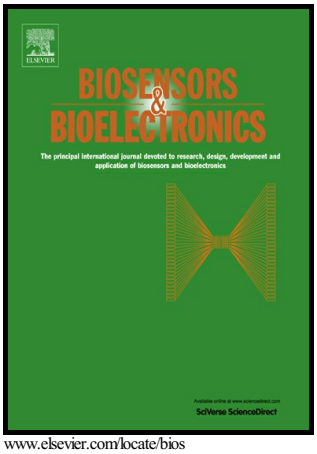

www.elsevier.com/locate/bios

Novel strategy for sulfapyridine detection using a fully integrated electrochemical Bio-MEMS: Application to honey analysis

Nadia El Alami El Hassani, Abdoullatif Baraket, Ernandes Taveira Tenório Neto, Michael Lee, Juan Pablo Salvador, Maria pilar Marco Colas, Joan Bausells, Nezha El Bari, Benachir Bouchikhi, Abdelhamid Elaissari, Abdelhamid Errachid, Nadia Zine

PII: S0956-5663(16)30840-5
DOI: http://dx.doi.org/10.1016/j.bios.2016.08.083
Reference: BIOS9080

To appear in: *Biosensors and Bioelectronic*

Received date: 17 June 2016
Revised date: 17 August 2016
Accepted date: 25 August 2016

Cite this article as: Nadia El Alami El Hassani, Abdoullatif Baraket, Ernandes Taveira Tenório Neto, Michael Lee, Juan Pablo Salvador, Maria pilar Marco Colas, Joan Bausells, Nezha El Bari, Benachir Bouchikhi, Abdelhamid Elaissari Abdelhamid Errachid and Nadia Zine, Novel strategy for sulfapyridine detection using a fully integrated electrochemical Bio-MEMS: Application to honey analysis, *Biosensors and Bioelectronic* http://dx.doi.org/10.1016/j.bios.2016.08.083

Novel strategy for sulfapyridine detection using a fully integrated electrochemical Bio-MEMS: Application to honey analysis

Nadia El Alami El Hassani [a,b,c], Abdoullatif Baraket [c], Ernandes Taveira Tenório Neto [d], Michael Lee [c], Juan Pablo Salvador [e], Maria pilar Marco Colas [e], Joan Bausells [f], Nezha El Bari [a], Benachir Bouchikhi [b], Abdelhamid Elaissari [d], Abdelhamid Errachid [c], Nadia Zine [c]

[a] Biotechnology Agroalimentary and Biomedical Analysis Group , Department of Biology, Faculty of Sciences, Moulay Ismaïl University, BP 11201, Zitoune, Meknes, Morocco
[b] Sensor Electronic and Instrumentation Group, Department of Physics, Faculty of Sciences, Moulay Ismail University, BP 11201, Zitoune, Meknes, Morocco
[c] Université de Lyon, Institut des Sciences Analytiques, UMR 5280, CNRS, Université Lyon 1, ENS Lyon - 5, rue de la Doua, F-69100 Villeurbanne, France
[d] Université de Lyon, LAGEP, UMR-5007, CNRS, Université Lyon 1, 5007, 43 Bd 11 Novembre 1918, F-69622 Villeurbanne, France.
[e] Institute of Advanced Chemistry of Catalonia, Department of Chemical and Biomolecular Nanotechnology, C/ Jordi Girona 18-26 08034, Barcelona, Spain.
[f] Instituto de Microelectronica de Barcelona, IMB-CNM (CSIC) Campus UAB, 08193, Bellaterra, Barcelona, Spain.
Corresponding author: E-mail address: nadia.zine@univ-lyon1.fr

Abstract:

Sulfapyridine (SPy) is a sulfonamide antibiotic largely employed as veterinary drugs for prophylactic and therapeutic purposes. Therefore, its spread in the food products has to be restricted. Herein, we report the synthesis and characterization of a novel electrochemical biosensor based on gold microelectrodes modified with a new structure of magnetic nanoparticles (MNPs) coated with poly(pyrrole-*co*-pyrrole-2-carboxylic acid) (Py/Py-COOH) for high efficient detection of SPy. This analyte was quantified through a competitive detection procedure with 5-[4-(amino)phenylsulfonamide]-5-oxopentanoic acid-BSA (SA2-BSA) antigens toward polyclonal antibody (Ab-155). Initially, gold working electrodes (WEs) of integrated biomicro electro-mechanical system (BioMEMS) were functionalized by Ppy-COOH/MNPs, using a chronoamperometric (CA) electrodeposition. Afterward, SA2-BSA was covalently bonded to Py/Py-COOH/MNP modified gold WEs through amide bonding. The competitive detection of the analyte was made by a mixture of a fixed concentration of Ab-155 and decreasing concentrations of SPy from 50 µg L^{-1} to 2 ng L^{-1}. Atomic Force Microscopy characterization was performed in order to ensure Ppy-COOH/MNPs electrodeposition on the microelectrode surfaces. Electrochemical measurements of SPy detection were carried out using electrochemical impedance spectroscopy (EIS). This biosensor was found to be highly sensitive and specific for SPy, with a limit of detection of 0.4 ng L^{-1}. This technique was exploited to detect SPy in honey samples by using the standard addition method. The measurements were highly reproducible for detection and interferences namely, sulfadiazine (SDz), sulfathiazole (STz) and sulfamerazine (SMz). Taking these advantages of sensitivity, specificity, and low cost, our system provides a new horizon for development of advanced immunoassays in industrial food control.

Keywords:
BioMEMS, Magnetic nanoparticles (MNP), Biosensor, Sulfapyridine, Food control.

1. Introduction

Sulfonamides are amongst the most important drugs used to treat and in some cases prevent bacterial infection. Nevertheless, their effectiveness and easy access led to overuse, prompting bacteria to develop resistance phenomenon (Maddocks and Jenkins 2013) and

leading to a decrease in their efficiency of treating human or animal diseases (Fernández et al. 2010). Around 30 sulfonamides are commercially available and prevalently in clinical uses (Jia et al. 2011), some of them with good growth-promoter effects, which help to overcome the challenges of managing animal health and food safety (Cheong et al. 2010).
Sulfapyridine (SPy) is one of the most widely used sulfonamides, which have been largely employed as veterinary drugs for prophylactic and therapeutic purposes. Therefore, its spread in the environment has to be restricted.

To limit human exposure to antibiotics, the European Union (EU) defined that the residue content of SPy in edible tissues and milk should not be higher than 100 $\mu g.kg^{-1}$ (Regulation (EC) No.470/2009). Honey is a particular case concerning the maximum level of SPy residues, since its treatment with antibiotics is banned in the EU. Thus, no maximum residue limits of antibiotics have been yet established (Kivrak et al. 2016), even if there is always a need to use it in order to prevent and to combat the bacterial diseases of honeybees (Dubreil-Cheneau et al. 2014). For this interest, and assuming that antibiotics are used to treat hive diseases, some countries, such as, Switzerland, UK, and Belgium, have set residues limits for SPy ranging from 10 to 50 $\mu g\ kg^{-1}$ (Bargańska et al. 2011).

However, the detection of antibiotic residues at low concentrations in animal products requires highly efficient sample preparation steps. Various analytical methods currently exist for the detection and quantification of SPy. Enzyme immunoassay, (Galarini et al. 2014; Jiang et al. 2013), high-performance liquid chromatography (HPLC) (Qi et al. 2015; Zhang et al. 2016), and liquid chromatography-mass spectroscopy (LC-MS) (Dubreil-Cheneau et al. 2014; Herrera-Herrera et al. 2013) have been described for confirmatory analysis. Most of these methods usually involve the use of extraction procedures, such as liquid–liquid (Dubreil-Cheneau et al. 2014) and solid phase (Juan-Borrás et al. 2015), to promote both the sample cleanup and analytes pre-concentration. Nevertheless, this two-stage procedure presents some prominent disadvantages such as the high costs, long time of execution and professional technical skills (Joshi and Anderson 2012).
Therefore, within the last decade, it has been demonstrated that optical and electrochemical immunosensors can be excellent tools to detect contaminants in food, environmental matrices and biomedical applications (Bougrini et al. 2016; Dmitrienko et al. 2014). They have revolutionized modern analysis because of their technical simplicity, low cost and the possibility of being employed in field analysis.
Electrochemical biosensors based on the use of receptors fabricated through different imprinting approaches have been developed for the detection of SPy (Conzuelo et al. 2012; Muriano et al. 2013). Furthermore, a coulombimetric immunosensor for SPy detection in honey has been developed by (Valera et al. 2013); the limit of detection was 0.11 $\mu g\ kg^{-1}$.
In a few articles (Song et al. 2012), the application of aptamer-based sensors and assays for the detection of sulfonamides has been mentioned and successfully applied to the analysis of milk samples. In addition to the methods described above, different physicochemical approaches have been used. They include fluorescence, spectrophotometry, surface enhanced Raman spectroscopy and electrochemical methods (Dmitrienko et al. 2014). Recently, lab-on-a-chip has been suggested as a perfect medium for portable and real-time food contaminant detection and for biomedical application (Baraket et al. 2016; Yoon and Kim 2012).
In this work, an alternative procedure is proposed for residual SPy detection in honey. In order to obtain such objective, our approach consists of the development of highly sensitive bio-micro-electro-mechanical systems (Bio-MEMS) transducers for the detection of SPy at low ppb concentration level. The quantification of SPy was achieved through competitive procedure with SA2-BSA immobilized on the WEs surface toward antibodies Ab-155. The developed bioMEMS is based on gold WEs functionalized with magnetic nanoparticles coated poly(pyrrole-*co*-carboxylic acid) (Py/Py-COOH/MNP). The use of polypyrrole copolymer is for detection signal enhancement via sensor surface modification. Whereas, the

magnetic property will be of great importance for bio-conjugates preparation, magnetic assisted biosensor surface modification. The magnetic property of the submicron functional magnetic particles can also be used as a carrier in microfluidic systems integrating biosensor for detection. Then, in this case, sample preparation and detection will be performed sequentially. These two last points will not be addressed in this work. The quantification of SPy was achieved through competitive procedure with SA2-BSA immobilized on the WEs surface toward specific antibodies Ab-155.

2. Experimental

2.1 Reagents and solutions

Pyrrole (98 %, Py), povidone (PVP), pyrrole-2-carboxylic acid (Py-COOH) 99 %, iron chloride hexahydrate 97 % ($FeCl_3 \cdot 6H_2O$), Sulfapyridine (SPy), Sulfadiazine (SDz), Sulfathiazole (STz), Sulfamerazine (SMz), 1-Ethyl-3-(3-dimethylaminopropyl)carbodiimide (EDC), Ethanolamine (ETA), Pure ethanol (99.8 %), Potassium hexacyanoferrate II, Potassium hexacyanoferrate III, Tween 20, Phosphate buffer saline (PBS) with pH 7.4 were all purchased from Sigma–Aldrich. Pyrrole was purified by passing through a column of activated basic alumina (Acros) before use. N-Hydroxysuccinimide (NHS) was purchased from Acros Organics. 5-[4-(amino)phenylsulfonamide]-5-oxopentanoic acid-bovine serum albumin (SA2-BSA) antigen, the sulfonamide class-selective polyclonal antiserum (Ab-155) raised against SA2 and Rabbit polyclonal Estrogen Receptor-beta (Ab-87) antibody were supplied by Institute for Advanced Chemistry of Catalonia. The oil-in-water magnetic emulsion (ME) (total solid content 7.9 %) consisted of magnetite nanoparticles stabilized with oleic acid, octane, and dodecyl sodium sulfate was acquired from Ademtech S. A. (lot E5 255b-2). Rosemary honey sample, guaranteed sulfonamides-free was supplied by Secrets d'Apiculteur, Lyon, France. Honey sample with unknown concentration of SPy was commercially provided.

2.2 Process for Bio-MEMS fabrication

The BioMEMS based on gold microelectrodes were fabricated onto silicon wafers of 100 mm diameter. Silicon dioxide (SiO_2) was grown at 800 nm by wet thermal oxidation. Afterward, gold working microelectrodes were defined by deposition and patterning of a metal tri-layer of Ti (100 nm), Ni (150 nm), and Au (50 nm). For the counter microelectrode, a bilayer of Ti (15 nm) plus Pt (150 nm) were deposited, and patterned by a lift-off process. This was followed by a dielectric passivation layer, obtained by plasma-enhanced chemical vapor deposition (PECVD) of SiO_2 (400 nm) plus Si_3N_4 (400 nm). The passivation layer was eliminated from all the microelectrode areas and the contact pads. Finally for the reference integrated microelectrode, a bilayer of Ti (15 nm) plus Ag (150 nm) was deposited and patterned by lift-off.

2.3 Synthesis of magnetic nanoparticles-coated with poly(pyrrole-*co*-pyrrole-2-carboxylic acid) (Py/Py-COOH/MNP)

Magnetic nanoparticles were synthesized using a seeded-polymerization technique (Tenorio-Neto et al. 2016). Briefly, the seeded-polymerization was carried out in a 25 mL glass reactor using a Teflon paddle stirrer. Then, 1.52 g of magnetic emulsion (ME) (0.12 g dried extract) was weighed, and added into the reactor. The supernatant was removed after 5 min of magnetic separation. After that, 10 mL of aqueous solution containing 20 mg of povidone (stabilizing agent) was added into reactor and ME was re-dispersed under continuous stirring (300 rpm) for 4 h. Afterward, 8.5 µL of Py (16 mmol) and 18 mg of Py-

COOH (16 mmol) were added into the reactor with 90 mg $FeCl_3.6H_2O$ (initiator). The reaction was kept under stirring during 12 h at room temperature.

2.4 Process for biosensor Bio-functionalization

Fig. 1A shows the image of the BioMEMS used in this work. The chip includes eight integrated gold WEs (225 µm²), Ag/AgCl reference microelectrode ((RE) 2908/180 µm) and platinum counter microelectrode ((CE) 1980/480µm).
Firstly the chips were cleaned with UV-Ozone (UV-Ozone Cleaner–ProCleaner™ Plus from BioForce) for 30 min to remove all organic contaminants.

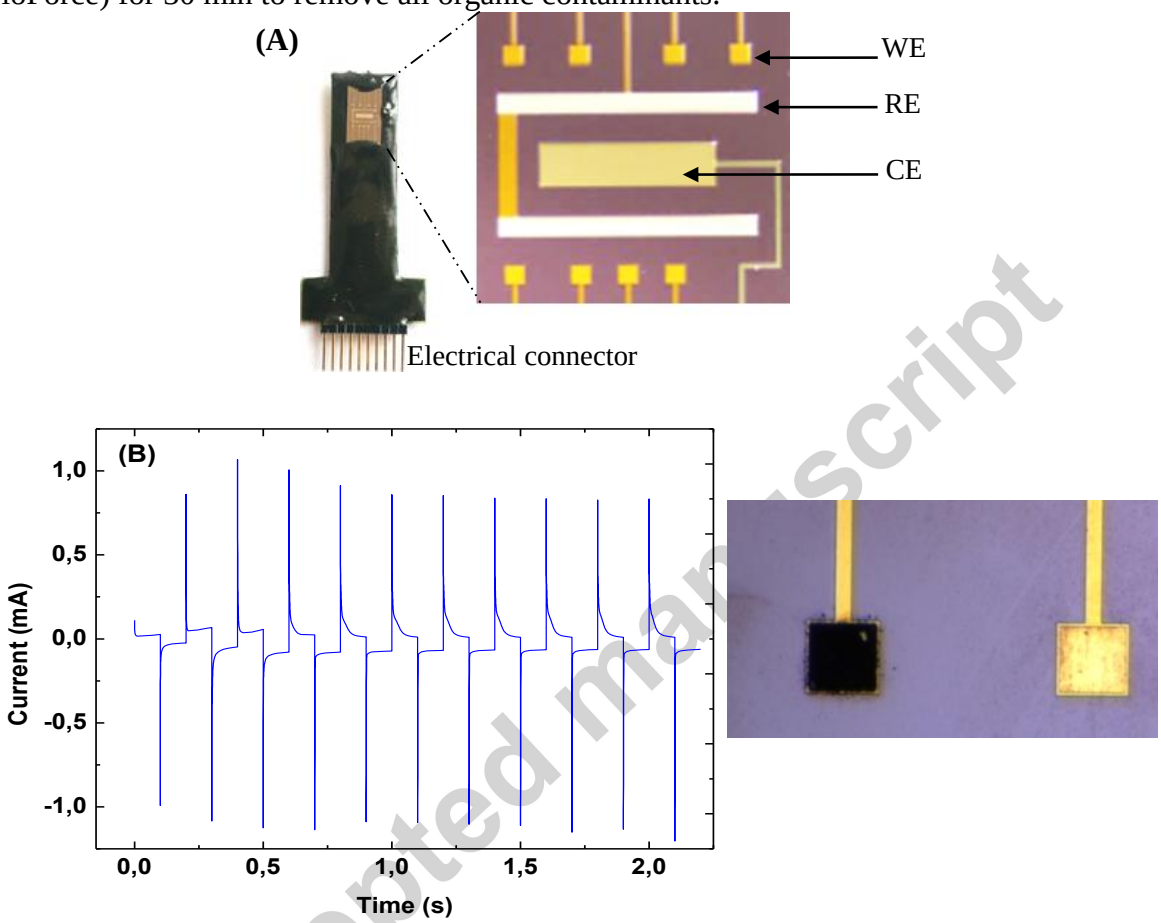

Fig. 1. (A) A full optical image of the final BioMEMS after packaging and a magnification onto the window of analysis with eight gold WEs, RE and CE, (B) Current density/time profiles for pulsed electrodeposition mode of Py/Py-COOH/MNP, (C) Stereo-microscopic image of Py/Py-COOH/MNP modified gold WE (Black) compared to bare gold WE (yellow).

Afterwards, Py/Py-COOH/MNP were electrodeposited onto WEs by using pulsed chronoamperometric (PCA) technique. Here two continuous repetition potentials were been applied: the first potential $E_1 = -1.5$ V for $t_1 = 0.1$ s, induces a cathodic electrodeposition process, while the second potential $E_2 = 1.0$ V for $t_2 = 0.1$ s oxidizes the surface electrode, and in particular, cleans it from eventual extraneous deposited species. The cycling process was iterated 10 times (Fig. 1B). Then, the gold WEs were rinsed with distilled water. In addition, it is interesting to point out that the amplitude of the charge–discharge process remains practically unchanged during the prolonged cycling process, indicating that the electrode surface exhibits an homogenous Py/Py-COOH/MNP deposition (Fig. 1C).
In order to activate the carboxylic groups, present in the Py/Py-COOH/MNP, the modified microelectrodes were treated with a mixture of 0.4 M EDC and 0.1 M NHS, prepared in

ethanol for 1 hour at room temperatureAfterward, the sensor was incubated in 40 µL of SA2-BSA at 100 µg mL^{-1} for 30 min at room temperature (Fig. 2). The details of synthesis of SA2-BSA were described in the literature (Adrian et al. 2009).

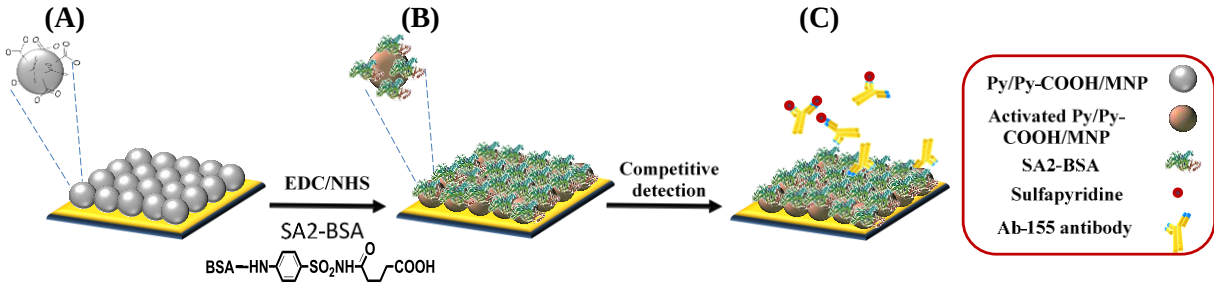

Fig. 2. Schematic representation of the gold WE functionalization based on (A) Py/Py-COOH/MNPs (B) SA2-BSA, and (C) the competitive detection of SPy by Ab-155 antibody.

Then, the biosensor was treated with ethanolamine (1 % v/v) in PBS buffer (pH = 7.4) for 10 min at room temperature, in order to deactivate the unbound sites. This step is very important to prevent nonspecific bonding phenomenon at the detection stage. Finally, the biosensor was rinsed with PBS and used for SPy detection.

2.5 Atomic force microscopy (AFM)

The surface topology and the roughness of the polymer film were investigated using atomic force microscopy (AFM), with a maximum area of scan is 110 μm^2. Measurements were made using silicon cantilever tip (ScienTecAppNano). The cantilever size was as follows: (L) = 125 µm, (W) = 35 µm and (T) = 4.5 µm for length, width and thickness respectively. The tip radius was ≤ 10 nm and the tip height (H) = 14-16 µm, with a frequency ranged between 200-400 kHz and a tip strength of K= 25-75 N/m. The scanning images were performed at 5 V amplitude, 8 V set point and tip direct current at 477 nV. Measurements were performed in taping mode with a speed of 0.5 lines/s and a resolution of 1024 lines. Samples were analyzed in a 5.0 µm × 4.4 µm area.

2.6 Electrochemical measurements

All steps of gold WEs modification were characterized by cyclic voltammetry (CV) and electrochemical impedance spectroscopy (EIS) techniques using a multi-channel potentiosat (VMP3 Bio-logic-Science Instrumentation (France)). The electrochemical configuration was performed by using integrated WEs, RE and CE of the BioMEMS. All the measurements were performed in a solution of 5.0 mM $[Fe(CN)_6]^{3-/4-}$ prepared in PBS buffer (pH= 7.4) and in a Faraday cage. For the cyclic voltammetric measurements, the potential was scanned from -0.3 V to 0.6 V with a scan rate of 100 mV s^{-1}. While the electrochemical impedance was measured, in the 200 mHz - 200 kHz frequency range, with a DC potential of 0.228 V/ref and a AC potential of 25 mV.

3. Results and discussion

3.1 Characterization of Py/Py-COOH/MNP

The prepared magnetic particles containing Py-COOH are characterized using various complementary techniques. The hydrodynamic particles size was first determined using dynamic light scattering and found to be around 277 nm with narrow size distribution in

nature. The zeta potential deduced from electrophoretic mobility measurement was found to be negative irrespective of pH (Fig. S1) (Supplementary data), reflecting the negative character of the particles surface due to the presence of carboxylic groups.

The morphology of the prepared Py/Py-COOH/MNP was examined using transmission electron microscopy (TEM). As can be seen from TEM image (Fig. S2) (Supplementary data), the particles are spherical and core-shell in nature, with magnetic core and poly(pyrrole-*co*-pyrrole carboxylic acid) shell. In addition, the particles are not smooth but surface roughness is attributed to local surface polymerization.

The chemical composition of the used magnetic polypyrrole particles was performed using thermogravimetric analysis. As can be seen in Fig. S3 (Supplementary data), the residual mass decreases with increasing temperature before reaching 45 % of residual mass attributed to iron oxide. Whereas, 55 % of organic material can be attributed to the use of surfactant for seed magnetic emulsion preparation, and the use of polymer shell.

FT-IR analysis of the used magnetic conducting carboxylic particles was examined and the obtained results are reported in Fig. S4 (Supplementary data). The presence of peaks between 1700 cm^{-1} to 1600 cm^{-1} can be attributed to C=O stretching from Py-COOH segments and also to the carbonyl groups of oleic acid used in the formulation of seed magnetic particles (Tenorio-Neto et al. 2016).

3.2 Atomic Force Microscopy (AFM)

After the electrochemical deposition of Py/Py-COOH/MNP film, AFM characterization was performed in order to check the homogeneity and the roughness of the WE surface. The two dimensional (2D) surface topography of Py/Py-COOH/MNP film (Fig. 3A) shows the typical porous granular morphology. The surface was totally homogenous and shows the presence of spherical shapes indicating the presence of MNP coated with Py/Py-COOH. This was clearly observed in the three-dimensional (3D) surface topography with a surface roughness of 8.4 nm (Fig. 3B). The AFM characterization was made to make sure that Py/Py-COOH/MNP were well immobilized onto the surface before antigen immobilization.

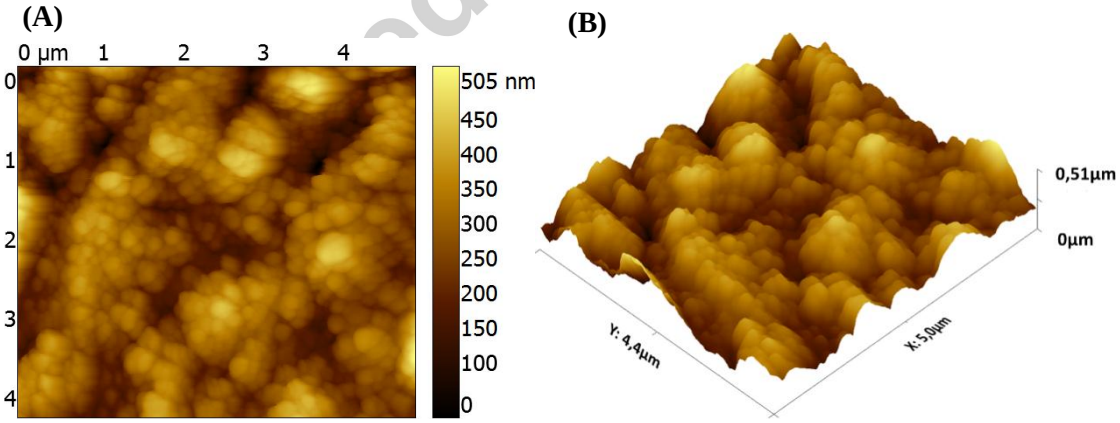

Fig. 3. AFM images of Py/Py-COOH/MNP -modified gold surface: (A) two dimensional (2D) surface topography (B). Three-dimensional (3D) surface topography. The dimensions of the image in X and Y coordinates are in the range of 5.0 µm × 4.4 µm.

3.3 Electrochemical characterization of Py/Py-COOH/MNP modified gold microelectrodes

To characterize the behavior of Py/Py-COOH/MNP layer, CV and EIS analysis have been performed for each step of the bioMEMS bio-functionalization. Fig. S5A (Supplementary data) shows cyclic voltammograms where the redox peaks have greatly increased after Py/Py-COOH/MNP deposition when compared to bare gold. This was due to the conductive properties of poly(pyrrole-co-pyrrole-2-carboxylic acid) coated on MNP. This was confirmed by EIS analysis (Fig. S5B) (Supplementary data) where the Nyquist plot semi-circle has significantly decreased when compared to bare gold indicating thus a faster charge-transfer kinetics as compared to that of bare electrode. At this stage the modified gold WE microelectrodes was ready for bio-functionalization.

3.4 Optimization of Ab-155 antibody concentration

Aiming the high sensitivity of Spy detection, the optimum concentration of the antibodies, which will react completely with the SA2-BSA (100 µg mL^{-1}) on gold electrode, was previously optimized by EIS analysis before the detection process. Fig. S6 (Supplementary data) shows the impedance spectra of the functionalized gold microelectrode corresponding to the interaction antigen-antibody for different concentrations of Ab-155 antibody. Here, the SA2-BSA modified WE shows a saturation at 10 µg mL^{-1} of Ab-155. This concentration was the minimum that can saturate the surface and it will be used for all the rest of the competitive detection of SPy.

Generally for the immunosensors, the antibodies are immobilized first and afterward the antigens are detected at different concentrations (Conzuelo et al. 2014). It is worth to mention that in the present study, the technology of detection has been inversed by adopting a competitive technique between the coating antigens (SA2-BSA) and the target antibiotics (SPy) in solution with the corresponding antibodies (Ab-155). This approach has been made due to the small molecular weight of SPy (249 Da) when compared to Ab-155 (150 kDa). Therefore, if the antibodies Ab-155 were immobilized onto gold WEs, the signal of SPy detection at minute concentration will be negligible. Moreover, this approach was privileged in our study to make pre-concentration to detect only SPy and eliminate other extraneous substances.

3.5 Competitive detection between SA2-BSA and SPy

The quantification of SPy antigens at various concentrations is shown in Fig. 4A. This step was carried out by incubating the bioMEMS surface in a mixture of a fixed concentration of Ab-155 (10 µg mL^{-1}) and a decreasing concentrations of SPy solutions (50 µg L^{-1} - 2 ng L^{-1}) in PBS buffer during 30 min at 4 °C for each concentration. Finally, the electrode was rinsed with PBST (10 mM PBS with 0.05 % Tween 20) and analyzed with EIS. At least three independent replicated experiments were performed. As it can be seen in Fig. 4A, the Nyquist plot semi-circles increase by decreasing SPy concentrations. As expected, the decrease of SPy concentration produces an increase in the charge transfer resistance due to presence of free antibodies that react with SA2-BSA.

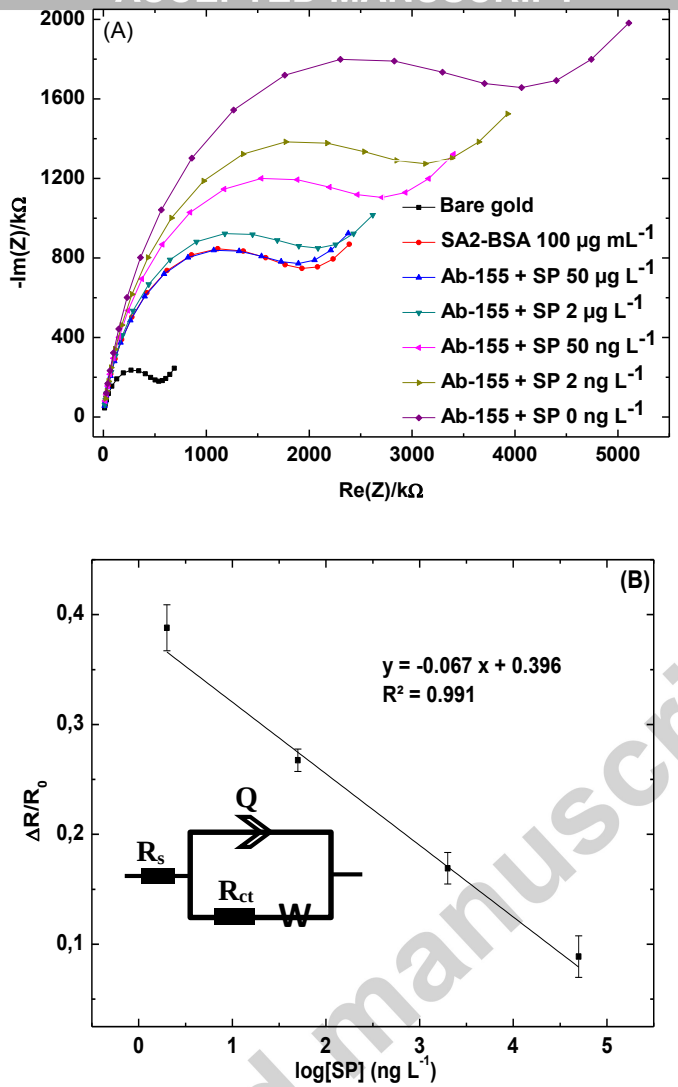

Fig. 4. (A) Nyquist impedance plots in 5 mM of $[Fe(CN)_6]^{3-/4-}$ for competitive detection of SPy at different concentration. Frequency range: 200 mHz to 200 kHz. DC potential: 0.228 V/ref and AC potential: 25 mV. (B) The sensitivity of the biosensor by normalization of Nyquist plot data Inset: the equivalent circuit used for EIS fitting, where R_s is the solution resistance, R_{ct} is the charge-transfer resistance, W is the Warburg impedance, and Q is the constant phase element.

The Nyquist plot semi-circles have been fitted with EC-Lab software using the Randles equivalent circuit shown in the inset of Fig. 4B. An excellent fitting between the simulated and experimental spectra was obtained for each SPy concentrations, and the equivalent circuit parameters are presented in Table S1 (Supplementary data).

The value of $\Delta R/R_0$ was calculated for each SPy concentration. The normalized data shows a linear equation: y = -0.067 x + 0.396, with a correlation coefficient of 0.991 (Fig. 4B).The limit of detection (LOD) for this biosensor, is found to be 0.4 ng L^{-1}. It is interesting to highlight that this LOD value is approximately 25000 times lower than the limits of SPy in honey fixed by Switzerland, UK and Belgium legislation. Therefore, these results are promising for the application of the developed biosensor in the control of SPy in foods such as honey. The comparison of the LOD between the proposed biosensor and other published studies was listed in Table 1. The result indicated that this system enabled relatively wide linear ranges and low LODs.

Table 1 Comparison of various technics for SPy detection.

Methods	Linear range (ng mL^{-1})	LOD (ng mL^{-1})	Real sample	Reference
High-performance liquid-chromatography with fluorescence detection	2-200	0.8	Honey	Tsai et al. 2010
High-pressure liquid chromatography /tandem mass spectrometry	0.006-0.250	0.012	River water	Iglesias et al. 2012
Amperometric immunosensor	0.6-64.2	0.15	Milk	Conzuelo et al. 2012
Scanning Electrochemical Microscopy	0.5-56.0	0.13	Milk	Conzuelo et al. 2014a
A biofuel cell consisting of a self-powered immunosensor	5-55	2.4	Milk	Conzuelo et al. 2014b
Optical immunosensor	0.7–21.0	0.2	Milk	Adrian et al. 2009
Competitive indirect enzyme-linked immunosorbent assay	1.05–10.45	1.15	Swine urine and milk	Liu et al. 2012
Electrochemical magneto-immunosensor	0.2-32.0	0.07	Honey	Muriano et al. 2013
Coulombimetric immunosensor	0-100	0.018	Honey	Valera et al. 2013
Electrochemical sensor	1.5–40.1	12.3	Human plasma	Ghoreishi et al. 2013
This work	0.002-50	0.0004	Honey	-

3.6 Selectivity study

Biosensor selectivity must be verified experimentally, due to the cross-reactivity that the Ab-155 antibodies may have with the antibiotics from the same family of sulfonamides. The selectivity of the present bioMEMS was investigated by comparing its responses to another sulfonamides with analogous structures namely sulfadiazine (SDz), sulfathiazole (STz), and sulfamerazine (SMz). EIS analyses were performed, using the same experimental process based on Py/Py-COOH/MNP/SA2-BSA immobilization. The detection of SDz, STz and SMz was made by the competitive method in the same range of concentrations from 50 µg L^{-1} to 2 ng L^{-1}. For the different interference antibiotics, we have obtained a calibration curves with a lower slopes compared to SPy, indicating that the biosensor displays the best selectivity to this latter (Fig. S7) (Supplementary data). Moreover, a slight response was observed for STz, SDz, due to the similarities between their chemical formulas, whereas, there is a negligible

response to SMz, which can be due to the presence of its terminal methyl group. Therefore, the biosensor has a good selectivity to SPy antibiotics, and can offer credible results despite the presence of the interfering species.

3.7 Application to the analysis of spiked honey samples: recovery study

A recovery study was performed by the standard addition technique by spiking honey sample with the target antibiotic. Honey samples were prepared as follows: 1 g of honey free of SPy was dissolved with 1 mL of ethanol in order to release SPy-sugar conjugates through the amino group in the aniline ring, and kept in an ultrasonic bath for 20 min. For reducing the matrix effect, the honey solution was diluted with PBS (1:10, v/v) (Valera et al. 2013). The solution was then spiked with different mixtures of Ab-155 and SPy within the dynamic range previously described. The comparison of the spiked concentrations and the determined concentrations were listed in Table S2 (Supplementary data). Recoveries from 73 % to 94 % were found, with a RSD ranging between 1 % and of 15 %. This indicates that the proposed biosensors can be used to detect SPy residues in real matrix with acceptable repeatability.

3.8 Detection of SPy in unknown honey sample

A standard addition technique was applied to measure the concentration of SPy in an unknown honey sample. Firstly, the honey sample was diluted 10 times in PBS. Then, different aliquots were taken and mixed with different concentrations of standard SPy solutions (50 ng L^{-1}, 30 ng L^{-1}, 10 ng L^{-1}, and 2 ng L^{-1}) in the presence of Ab-155 (10 µg mL^{-1}). For each aliquots containing SPy, the normalized charge transfer resistance $\Delta R/R_0$ were measured. The unknown concentration in the diluted sample (obtained from the extrapolated of the regression line Fig. 5a) was found to be 6.97 ng L^{-1}. Therefore, the concentration of SPy in the unknown sample was 69.7 ng L^{-1}. This concentration remains lower from the limit of residues, set by Switzerland, UK and Belgium.

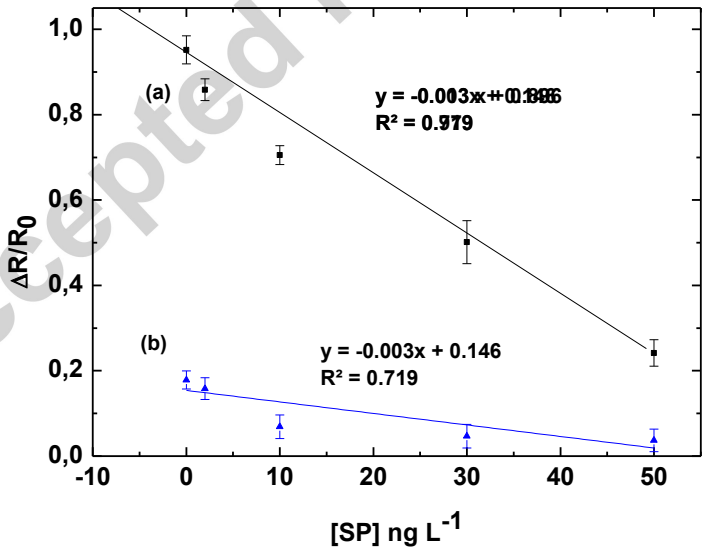

Fig. 5. Standard addition plot of different SPy spiking in diluted unknown honey sample, using (a) Ab-155 and (b) Ab-87 antibodies.

In order to confirm these results a negative test was performed using the same previous standard added volume method with another antibodies Ab-87 instead Ab-155. Therefore, different solutions from diluted honey in PBS (1:10, v/v) were mixed with different

concentrations of standard SPy solutions (50 ng L^{-1}, 30 ng L^{-1}, 10 ng L^{-1}, and 2 ng L^{-1}) with the presence of Ab-87 (10 µg mL^{-1}). Fig. 5b shows clearly the high sensitivity of the biosensor when using Ab-155 in comparison with Ab-87. This confirms that what was detected previously was well SPy and not a nonspecific adsorption.

4 Conclusion

Novel sensitive and selective biosensor based on new structure of MNP coated with poly(pyrrole-*co*-pyrrole-2-carboxylic acid) for the specific detection of SPy was developed. Py/Py-COOH/MNP was chosen for its 3D network of immobilization as well as its stability for long periods. Moreover, making electrochemical analysis using this material allows a stable measurement and rapid response. Under optimized conditions, the developed biosensor provides a high sensitivity of 0.067 L ng^{-1}, and a limit of detection of 0.4 ng L^{-1}. The biosensor was highly selective for SPy antigens, when compared to other interferences molecules namely sulfadiazine, sulfathiazole, and sulfamerazine. Moreover, the proposed biosensor offers a broad reliability to detect low levels of SPy residues in honey samples without any complex pre-treatment (just a dilution). The simplicity and miniaturization of this biosensor open the way to the development of a simple and inexpensive alternative biosensor in food control.

Acknowledgements

The authors acknowledge the financial support from PHC-Toubkal under the project No.32567YD, SEA-on-a-CHIP (FP7-OCEAN-2013) under the grant agreement No.614168, and funding from the European Union's Horizon 2020 research and innovation programme entitled HEARTEN under grant agreement No 643694" and microMole grant agreement No 643694 and No 653626 respectively.

References:

Adrian, J., Font, H., Diserens, J.-M., Sanchez-Baeza, F., Marco, M.-P., 2009. Journal of agricultural and food chemistry 57(2), 385-394.

Baraket, A., Lee, M., Zine, N., Yaakoubi, N., Bausells, J., Errachid, A., 2016. Microchimica Acta, 1-8.

Bargańska, Ż., Namieśnik, J., Ślebioda, M., 2011. TrAC Trends in Analytical Chemistry 30(7), 1035-1041.

Bougrini, M., Baraket, A., Jamshaid, T., El Aissari, A., Bausells, J., Zabala, M., El Bari, N., Bouchikhi, B., Jaffrezic-Renault, N., Abdelhamid, E., 2016. Sensors and Actuators B: Chemical 234, 446-452.

Cheong, C., Parvaneh, H., Selamat, J., Rashedi, M., Fitry, I., 2010. International Food Research Journal 17(4), 885-892.

Conzuelo, F., Gamella, M., Campuzano, S., Pinacho, D.G., Reviejo, A.J., Marco, M.P., Pingarron, J.M., 2012. Biosens Bioelectron 36(1), 81-88.

Conzuelo, F., Stratmann, L., Grützke, S., Pingarrón, J.M., Schuhmann, W., 2014a. Electroanalysis 26(3), 481-487.

Conzuelo, F., Vivekananthan, J., Pöller, S., Pingarrón, J.M., Schuhmann, W., 2014b. ChemElectroChem 1, 1854 – 1858.

Dmitrienko, S.G., Kochuk, E.V., Apyari, V.V., Tolmacheva, V.V., Zolotov, Y.A., 2014. Anal Chim Acta 850, 6-25.

Dubreil-Cheneau, E., Pirotais, Y., Verdon, E., Hurtaud-Pessel, D., 2014. J Chromatogr A 1339, 128-136.

Fernández, F., Hegnerová, K., Piliarik, M., Sanchez-Baeza, F., Homola, J., Marco, M.P., 2010. Biosensors and Bioelectronics 26(4), 1231-1238.

Galarini, R., Diana, F., Moretti, S., Puppini, B., Saluti, G., Persic, L., 2014. Food Control 35(1), 300-310.

Ghoreishi, S.M., Behpour, M., Khoobi, A., Masoum, S., 2014. Arabian Journal of Chemistry, In press

Herrera-Herrera, A.V., Hernandez-Borges, J., Borges-Miquel, T.M., Rodriguez-Delgado, M.A., 2013. J Pharm Biomed Anal 75, 130-137.

Iglesias, A., Nebot, C., Miranda, J.M., Vázquez, B.I., Cepeda, A., 2012. Environ Sci Pollut Res 19, 3235–3249

Jia, A., Hu, J., Wu, X., Peng, H., Wu, S., Dong, Z., 2011. Environ Toxicol Chem 30(6), 1252-1260.

Jiang, W., Wang, Z., Beier, R.C., Jiang, H., Wu, Y., Shen, J., 2013. Anal Chem 85(4), 1995-1999.

Joshi, M.D., Anderson, J.L., 2012. RSC Advances 2(13), 5470-5484.

Juan-Borrás, M., Periche, A., Domenech, E., Escriche, I., 2015. Food Control 50, 243-249.

Kivrak, I., Kivrak, Ş., Harmandar, M., 2016. Food Science and Technology (Campinas) 36(1), 90-96.

Liu, Na., Han, Z., Lu, L., Wang, L., Ni, G., Zhao, Z., Wu, A., Zheng, X., 2012. J Sci Food Agric

Maddocks, S.E., Jenkins, R.E., 2013. Future Microbiology 8(11), 1419-1429.

Muriano, A., Pinacho, D.G., Chabottaux, V., Diserens, J.M., Granier, B., Stead, S., Sanchez Baeza, F., Pividori, M.I., Marco, M.P., 2013. Anal Bioanal Chem 405(24), 7885-7895.

Qi, R., Lv, X., Niu, Q., Hu, B., Jia, Q., 2015. New Journal of Chemistry 39(8), 6323-6331.

Regulation (EC) 470/2009. Off. J. Eur. Commun., L152, 11-22.

Song, K.M., Jeong, E., Jeon, W., Jo, H., Ban, C., 2012. Biosens Bioelectron 33(1), 113-119.

Tenorio-Neto, E.T., Baraket, A., Kabbaj, D., Zine, N., Errachid, A., Fessi, H., Kunita, M.H., Elaissari, A., 2016. Mater Sci Eng C Mater Biol Appl 61, 688-694.

Tsai, W-H., Chuang, H-Y., Chen, H-H., Wu, Y-W., Cheng, S-H., Huang,T-C., 2010. J Chromatogr A 1217, 7812–7815.

Valera, E., Muriano, A., Pividori, I., Sanchez-Baeza, F., Marco, M.P., 2013. Biosens Bioelectron 43, 211-217.

Yoon, J.Y., Kim, B., 2012. Sensors 12(8), 10713-10741.

Zhang, Y., Liu, X., Li, X., Zhang, J., Cao, Y., Su, M., Shi, Z., Sun, H., 2016. Food Control 60, 667-676.

Highlights

- We manufactured a fully integrated electrochemical BioMEMS for sulfapyridine (Spy) detection.
- Polypyrrole-carboxylic acid (Py/Py-COOH) modified magnetic nanoparticles (MNP) were electrodeposited onto gold WEs.
- Electrochemical impedance spectroscopy (EIS) was used for competitive detection of SPy.
- The BioMEMS was highly sensitive and selective for SPy when compared to other sulfonamides antibiotics.

- This BioMEMS is very promising for multi-detection which can dramatically reduce time of analyses for food control applications.